HHS Public Access

Author manuscript

Cerebellum. Author manuscript; available in PMC 2021 July 23.

Published in final edited form as:

Cerebellum. 2018 October ; 17(5): 692–697. doi:10.1007/s12311-018-0950-5.

C-terminal proline deletions in *KCNC3* cause delayed channel inactivation and an adult-onset progressive SCA13 with spasticity

Swati Khare[1,2], **Kira Galeano**[3], **Yalan Zhang**[4], **Jerelyn A. Nick**[5], **Harry S. Nick**[5], **S. H. Subramony**[3], **Jacinda Sampson**[6], **Leonard K. Kaczmarek**[4], **Michael F. Waters**[2]

[1]Department of Biomedical Engineering, University of Florida, Gainesville, FL, USA

[2]Department of Neurology, Barrow Neurological Institute, St. Joseph's Hospital and Medical Center, 350 W. Thomas Rd., Phoenix, AZ 85013, USA

[3]Department of Neurology, University of Florida, Gainesville, FL, USA

[4]Department of Pharmacology, Yale University, New Haven, CT, USA

[5]Department of Neuroscience, University of Florida, Gainesville, FL, USA

[6]Department of Neurology, Stanford University, Stanford, CA, USA

Abstract

Mutations in the potassium channel gene *KCNC3* (Kv3.3) cause the autosomal dominant neurological disease, spinocerebellar ataxia 13 (SCA13). In this study, we expand the genotype-phenotype repertoire of SCA13 by describing the novel *KCNC3* deletion p.Pro583_Pro585del highlighting the allelic heterogeneity observed in SCA13 patients. We characterize adult-onset, progressive clinical symptoms of two afflicted kindred and introduce the symptom of profound spasticity not previously associated with the SCA13 phenotype. We also present molecular and electrophysiological characterizations of the mutant protein in mammalian cell culture. Mechanistically, the p.Pro583_Pro585del protein showed normal membrane trafficking with an altered electrophysiological profile, including slower inactivation and decreased sensitivity to the inactivation-accelerating effects of the actin depolymerizer latrunculin B. Taken together, our results highlight the clinical importance of the intracellular C-terminal portion of Kv3.3 and its association with ion channel function.

Michael F. Waters Michael.Waters@DignityHealth.org.

Electronic supplementary material The online version of this article (https://doi.org/10.1007/s12311-018-0950-5) contains supplementary material, which is available to authorized users.

All procedures performed in studies involving human participants were in accordance with the ethical standards of the institutional and/or national research committee and with the 1964 Helsinki declaration and its later amendments or comparable ethical standards.

Conflict of Interest The authors declare that they have no conflict of interest.

Ethical Approval Written informed consent was obtained from the patients for the publication of this study with approval from the Institutional Review Board (University of Florida and Columbia University). All procedures performed in studies involving human participants were in accordance with the ethical standards of the institutional and/or national research committee and with the 1964 Helsinki declaration and its later amendments or comparable ethical standards.

Keywords

Spinocerebellar ataxia 13; *KCNC3*; Spasticity; C-terminal deletion; Allelic heterogeneity

Introduction

Spinocerebellar ataxia 13 (SCA13) is a rare neurological disorder inherited in an autosomal dominant pattern. The clinical symptoms of SCA13 include classic SCA manifestations of ataxic gait and cerebellar atrophy along with tremor, seizures, hyperreflexia, nystagmus, cognitive impairment, dysarthria, and myoclonus [1–3]. SCA13 is caused by mutations in the potassium channel gene, *KCNC3* (MIM: 176264, Kv3.3). Kv3.3 channels are delayed rectifying voltage-gated potassium channels abundant in the Purkinje neurons of the cerebellum, where they contribute to high-frequency action potentials.

SCA13 mutations localize to different positions in the protein structure and display allelic heterogeneity with variations in age of onset, progression, and molecular and electrophysiological properties. The heterogeneity is exemplified by the two SCA13 mutations p.Arg420His [4] and p.Arg423His [5], both of which occur in the S4 transmembrane domain of Kv3.3. Though these mutations are only three amino acids apart and have identical substitutions, they manifest in fundamentally different ways: p.Arg420His results in late-onset, progressive disease, whereas p.Arg423His results in early-on-set, non-progressive disease. However, both mutant proteins are intracellularly retained in mammalian cell culture [6, 7]. Another SCA13 *KCNC3* mutation, p.Phe448Leu, leads to an early-onset form of SCA13, with the mutant protein trafficking normally to the membrane in cell culture. The p.Phe448Leu channel, however, shows abnormal shifts in activation voltages, further accentuating the phenotypic and pathophysiologic heterogeneity of SCA13 [1, 7].

A recent study has shown that the cytoplasmic C-terminal domain of Kv3.3 channels binds Hax-1, an anti-apoptotic protein required for the survival of cerebellar neurons [8]. One of the cellular functions of Hax-1 is to promote the Arp2/3-dependent nucleation of actin filaments. Accordingly, the binding of Hax-1 to Kv3.3 directly triggers the formation of a stable channel-associated subcortical actin cytoskeleton that acts to prevent inactivation of Kv3.3 during depolarization [8]. Disruption of this interaction with the actin-depolymerizing agent latrunculin B (LatB) causes the rapid inactivation of wild-type Kv3.3 channels. Another C-terminal *KCNC3* allele, p.Gly592Arg, prevents the channel from triggering actin nucleation [8]. In contrast to the mutations described in the previous paragraph, the electrophysiological properties of p.Gly592Arg channels are similar to those of wild-type Kv3.3, although their rate of inactivation is slower. Strikingly, the inactivation of these mutant channels is more resistant to the effects of LatB than that of the wild-type channels [8].

In the present study, we establish SCA13 causation from a novel deletion mutation of three proline residues, NM_004977.2: c.1746_54del, p.Pro583_Pro585del (Fig. 1(a)) in a region of the intracellular C-terminal domain of Kv3.3. We describe two affected pedigrees (Fig. 1(b,c)) to highlight overlapping and divergent phenotypes, and add to the symptoms of

SCA13 with the observation of marked spasticity. We further compare mechanistic features of this mutation with those of previously described SCA13 mutations.

Materials and Methods

Human Genetics and Imaging

DNA was isolated from patient blood (Qiagen, Hilden, Germany) or saliva (DNA Genotek, Ottawa, Canada) and sequenced at the University of Florida. Midline sagittal T1-weighted and axial magnetic resonance imaging (MRI) of patients were collected at the University of Florida (Gainesville, USA) or at Columbia University (New York, USA).

Cell Culture and Protein Analyses

The human *KCNC3* cDNA was provided by Dr. James L. Rae (Mayo Foundation). The p.Arg420His was generated as previously described [6]. The c.1746_54del (p.Pro583_Pro585del) mutant was generated in a pBKCMV vector with the In-Fusion HD Cloning kit (Clontech, Mountain View, USA). The *KCNC3* cDNA and both mutants were subcloned into pcDNA3-Clover (Addgene no. 40259, provided by Michael Lin). Flp-In-CHO (Thermo Fisher Scientific, Waltham, USA) cells were cultured and transiently transfected with pBKCMV or Clover tagged *KCNC3*, *KCNC3*-c.1259G>A (p.Arg420His), and *KCNC3*-c.1746_54del (p.Pro583_Pro585del), as previously described [5]. Immunoblotting, immunofluorescence, and live cell imaging were performed as described previously [5, 6].

Electrophysiology

Electrophysiology and statistics were performed in transfected CHO cells as previously described [8].

Results

Clinical Description

The family history of pedigree 583–1 (Fig. 1(b)) is reportedly negative for neurological abnormalities, with the father's death stated due to cardiac issues, and a genetically confirmed wild-type mother (583–1, I-1). The four sons had normal developmental milestones and no physical manifestations of disease from childhood to early adulthood.

Three of the siblings (Fig. 1(b) [583–1, II-2, II-3, II-4]) had physical manifestations that began in their early 30's and progressed (Fig. 1(b)). All three suffered from seizures; onset for all three (including the proband) was in their early 30's. Mild cognitive impairment subjectively described as dyslexia was noted in all three affected siblings. Examination of the proband (Fig. 1(b) [583–1, II-4]) at age 38 years revealed ambulation difficulty requiring assistive walking devices, frequent falls, limited upgaze, slow and hypometric saccades, dysarthria, dysphagia, impaired heel-to-shin coordination, tremor, and hyperreflexia in the legs greater than arms with non-sustained bilateral ankle clonus, normal strength, and marked appendicular spasticity in all four limbs, LE > UE (Supplementary Video 1). MRI of the proband showed marked cerebellar atrophy (Fig. 1(d)). Disease progression led to

dysmetria, impaired finger-to-nose coordination, incontinence, prominent cognitive impairment including declining memory, personality changes, emotional lability, and self-reported impaired judgment. Both of the probands' affected siblings died at the age of 49 years from aspiration pneumonia, despite placement of a percutaneous endogastric tube.

Electromyography, nerve conduction studies, and muscle biopsy of the proband were normal. Laboratory studies were unrevealing, including very long chain fatty acid, ceruloplasmin, copper, phytanic acid, vitamin B_{12}, vitamin E, anti-nuclear antibodies, erythrocyte sedimentation rate, thyroid-stimulating hormone, Lyme disease screen, and rapid plasma reagin. Genetic testing was negative for inherited ataxias (SCA 1, 2, 3, 6, 7, 8, Friedreich's, Pelizaeus-Merzbacher, dentatorubral-pallidoluysian atrophy, and hereditary spastic paraplegia type 1 or type 2) except for the heterozygous p.Pro583_Pro585del mutation in *KCNC3*, genetically confirmed in both II-4 and II-3. At age 46 years, the proband had a Scale for Assessment and Rating of Ataxia (SARA) [9] score of 21 and a Montreal Cognitive Assessment version 7.3 [10] score of 23, with primary deductions in language, memory, and delayed recall.

The proband in the second pedigree, 583–2 (Fig. 1(c), II-1), is positive for the p.Pro583_Pro585del *KCNC3* mutation and shows prominent cerebellar atrophy (Fig. 1(e,f)). She shows pure cerebellar signs of gait ataxia and incoordination that started in her 40's, although her cognition seems intact. Unlike the proband in 583–1, she has no notable spasticity, oculomotor, extrapyramidal, and upper or lower motor neuron deficits. Her SARA score increased from 8 to 10 over 24 months (Supplementary Table S1). Genetic testing of siblings II-2 and II-3 confirmed the absence of this variant in unaffected family members. One of her two children (III-2) is premanifest, while the other tested negative for the mutation.

Cellular and Electrophysiological Characterization

Previous studies have established aberrant glycosylation and protein mis-trafficking as features in the pathogenesis associated with the p.Arg420His and p.Arg423His *KCNC3* mutations [5–7]. Upon investigating the biochemical characteristics of p.Pro583_Pro585del, we found this mutant to be normally glycosylated, similar to the wild-type channel, and in contrast to p.Arg420His and p.Arg423His [6] (Fig. 2(a)). Correspondingly, immunofluorescence of KCNC3 (Fig. 2(b–d)) showed membrane localization of both the wild-type and p.Pro583_Pro585del proteins, in contrast to the intracellular retention of p.Arg420His and p.Arg423His [6]. Additionally, transient transfections of fluorescently tagged *KCNC3* constructs confirmed membrane localization f or bot h the wild-type and p.Pro583_Pro585del proteins (Fig. 2(e,f)), again in contrast to the retention of p.Arg420His and p.Arg423His [5] (Fig. 2(g)). Therefore, the p.Pro583_Pro585del protein demonstrated similarities to the mutant p.Phe448Leu and the wild-type protein by exhibiting normal glycosylation and intracellular trafficking.

A previous study indicated that the Kv3.3 channel-associated actin filaments are required to prevent channel inactivation [8]. Treatment with latrunculin B (LatB), an actin-depolymerizing agent, greatly increases the rate of inactivation of Kv3.3 channels during depolarization. We carried out whole-cell patch-clamp recordings on cells expressing

p.Pro583_Pro585del in the presence and absence of 10 μM LatB and compared their responses to those of cells expressing the wild-type protein (Fig. 3(a–c)). We found no difference in the voltage-dependence or the peak current amplitude of p.Pro583_Pro585del currents compared to those of wild-type Kv3.3 channels (Fig. 3(d,e)). The degree of inactivation produced by depolarization was, however, significantly reduced by the p.Pro583_Pro585del mutation, even in the absence of LatB. Inactivation was quantified by the ratio of current at the end of a 600-ms pulse (+ 70 mV) to the peak current at the onset of the pulse (Fig. 3(b–e)). Moreover, application of LatB accelerated the rate of inactivation in both wild-type and p.Pro583_Pro585del channels (Fig. 3(b,c)). The degree of inactivation was, however, significantly greater in wild-type channels than that in p.Pro583_Pro585del channels (Fig. 3(e)). These findings are similar to those described for the p.Gly592Arg allele [8].

Discussion

To summarize, we have expanded the genotype-phenotype-pathophysiology repertoire of SCA13 by addition of a causative *KCNC3* mutation, p.Pro583_Pro585del, its associated phenotype of profound spasticity, and the decreased inactivation rate of the mutant channel. This observation adds SCA13 to the limited group of autosomal dominant ataxias with spasticity as a symptom [11–14]. SCA13 shares many symptoms with other neurological diseases, making diagnosis challenging, as observed with a previous SCA13 patient who was mistakenly thought to have cerebral palsy [5]. The gnomAD *KCNC3*-p.Pro583_Pro585del allelic frequency of 10/161248 (0.00006202) may include SCA13 patients as one of the described families was initially reported from a diagnostic database. A complete description of symptoms is therefore essential to increase awareness and prevent misdiagnosis.

This form of SCA13 is phenotypically late-onset and progressive with notable differences in symptom severity between families. The proband of 583–1, II-4, displayed cerebellar symptoms of increased severity (SARA score 21), spasticity, and tremor with rapid and fatal progression, unlike the proband of 583–2, II-1, (SARA score 8–10) with slower progression. Genome-wide studies may provide insight on genetic modifiers potentially contributing to differences in disease severity.

The structure-function relationships of different regions of the Kv3.3 channel have not been described in detail, partly due to the lack of a crystal structure and minimal information on interacting partners. The difference in cellular trafficking behavior of this deletion mutant in contrast to the previously described mutations p.Arg423His and p.Arg420His implies that the C-terminal region of Kv3.3 may not play a key role in the channel’s trafficking.

Abnormalities in inactivation have previously been shown in association with the SCA13 mutation p.Arg423His [15], as well as in SCA3 mice where there is an increase in inactivation of Kv1 channels [16]. The electrophysiological characteristics of the p.Pro583_Pro585del mutant protein closely match those of the p.Gly592Arg allele in that it has a slower inactivation rate and is more resistant to disruption of the actin cytoskeleton [8]. Because Kv3.3 is linked to actin through Hax-1, a protein absolutely required for the

survival of cerebellar neurons [17], it is possible that cellular defects produced by these mutations affect the expression or trafficking of this cell survival protein. Future work can compare interacting partners of the wild-type and mutant p.Pro583_Pro585del, thereby providing valuable insight into the exact function of the C-terminal region of this channel. Our findings from this deletion mutation underscore the clinical relevance of the intracellular C-terminal portion of Kv3.3 and its association with ion channel function.

Supplementary Material

Refer to Web version on PubMed Central for supplementary material.

Acknowledgments

We thank the staff of Neuroscience Publications at Barrow Neurological Institute for assistance with manuscript preparation.

Funding Information Financial support was provided by NIH grants NINDS K23 NS054715 (M.F.W.), NIDCD01919 (L.K.K.), and the McKnight Brain Institute at the University of Florida.

References

1. Zhang Y, Kaczmarek LK. Kv3.3 potassium channels and spinocerebellar ataxia. J Physiol 2015;00:1–8.
2. Waters MF, Pulst SM. SCA13. Cerebellum 2008;7:165–9. [PubMed: 18592334]
3. Montaut S, Apartis E, Chanson JB, Ewenczyk C, Renaud M, Guissart C, et al. SCA13 causes dominantly inherited non-progressive myoclonus ataxia. Parkinsonism Relat Disord 2017;38:80–4. [PubMed: 28216058]
4. Waters MF, Minassian N, Stevanin G, Figueroa KP, Bannister JP, Nolte D, et al. Mutations in voltage-gated potassium channel KCNC3 cause degenerative and developmental central nervous system phenotypes. Nat Genet 2006;38:447–51. [PubMed: 16501573]
5. Khare S, Nick JA, Zhang Y, Galeano K, Butler B, Khoshbouei H, et al. A KCNC3 mutation causes a neurodevelopmental, non-progressive SCA13 subtype associated with dominant negative effects and aberrant EGFR trafficking. PLoS One 2017;12(5): e0173565. [PubMed: 28467418]
6. Gallego-Iradi C, Bickford JS, Khare S, Hall A, Nick JA, Salmasinia D, et al. KCNC3R420H, a K+ channel mutation causative in spinocerebellar ataxia 13 displays aberrant intracellular trafficking. Neurobiol Dis 2014;71:270–9. [PubMed: 25152487]
7. Duarri A, Nibbeling EA, Fokkens MR, Meijer M, Boerrigter M, Verschuuren-Bemelmans CC, et al. Functional analysis helps to define KCNC3 mutational spectrum in Dutch ataxia cases. PLoS One 2015;10(3):e0116599. [PubMed: 25756792]
8. Zhang Y, Zhang XF, Fleming MR, Amiri A, El-Hassar L, Surguchev AA, et al. Kv3.3 channels bind Hax-1 and Arp2/3 to assemble a stable local actin network that regulates channel gating. Cell 2016;165(2):434–48. [PubMed: 26997484]
9. Kim BR, Lim JH, Lee SA, Park S, Koh SE, Lee IS, et al. Usefulness of the scale for the assessment and rating of ataxia (SARA) in ataxic stroke patients. Ann Rehabil Med 2011;35(6):772–80. [PubMed: 22506205]
10. Nasreddine ZS, Phillips NA, Bedirian V, Charbonneau S, Whitehead V, Collin I, et al. The Montreal cognitive assessment, MoCA: a brief screening tool for mild cognitive impairment. J Am Geriatr Soc 2005;53:695–9. [PubMed: 15817019]
11. Pedroso JL, de Souza PV, Pinto WB, Braga-Neto P, Albuquerque MV, Saraiva-Pereira ML, et al. SCA1 patients may present as hereditary spastic paraplegia and must be included in spastic-ataxias group. Parkinsonism Relat Disord 2015;21(10):1243–6. [PubMed: 26231471]

12. Wang YG, Du J, Wang JL, Chen J, Chen C, Luo YY, et al. Six cases of SCA3/MJD patients that mimic hereditary spastic paraplegia in clinic. J Neurol Sci 2009;285(1–2):121–4. [PubMed: 19608203]

13. Koob MD, Moseley ML, Schut LJ, Benzow KA, Bird TD, Day JW, et al. An untranslated CTG expansion causes a novel form of spinocerebellar ataxia (SCA8). Nat Genet 1999;21(4):379–84. [PubMed: 10192387]

14. Tsoi H, Yu AC, Chen ZS, Ng NK, Chan AY, Yuen LY, et al. A novel missense mutation in CCDC88C activates the JNK pathway and causes a dominant form of spinocerebellar ataxia. J Med Genet 2014;51(9):590–5. [PubMed: 25062847]

15. Irie T, Matsuzaki Y, Sekino Y, Hirai H. Kv3.3 channels harbouring a mutation of spinocerebellar ataxia type 13 alter excitability and induce cell death in cultured cerebellar Purkinje cells. J Physiol 2014;592(1):229–47. [PubMed: 24218544]

16. Shakkottai VG, do Carmo Costa M, Dell'Orco JM, Sankaranarayanan A, Wulff H, Paulson HL. Early changes in cerebellar physiology accompany motor dysfunction in the polyglutamine disease spinocerebellar ataxia type 3. J Neurosci 2011;31(36):13002–14. [PubMed: 21900579]

17. Chao JR, Parganas E, Boyd K, Hong CY, Opferman JT, Ihle JN. Hax1-mediated processing of HtrA2 by Parl allows survival of lymphocytes and neurons. Nature 2008;452(7183):98–102. [PubMed: 18288109]

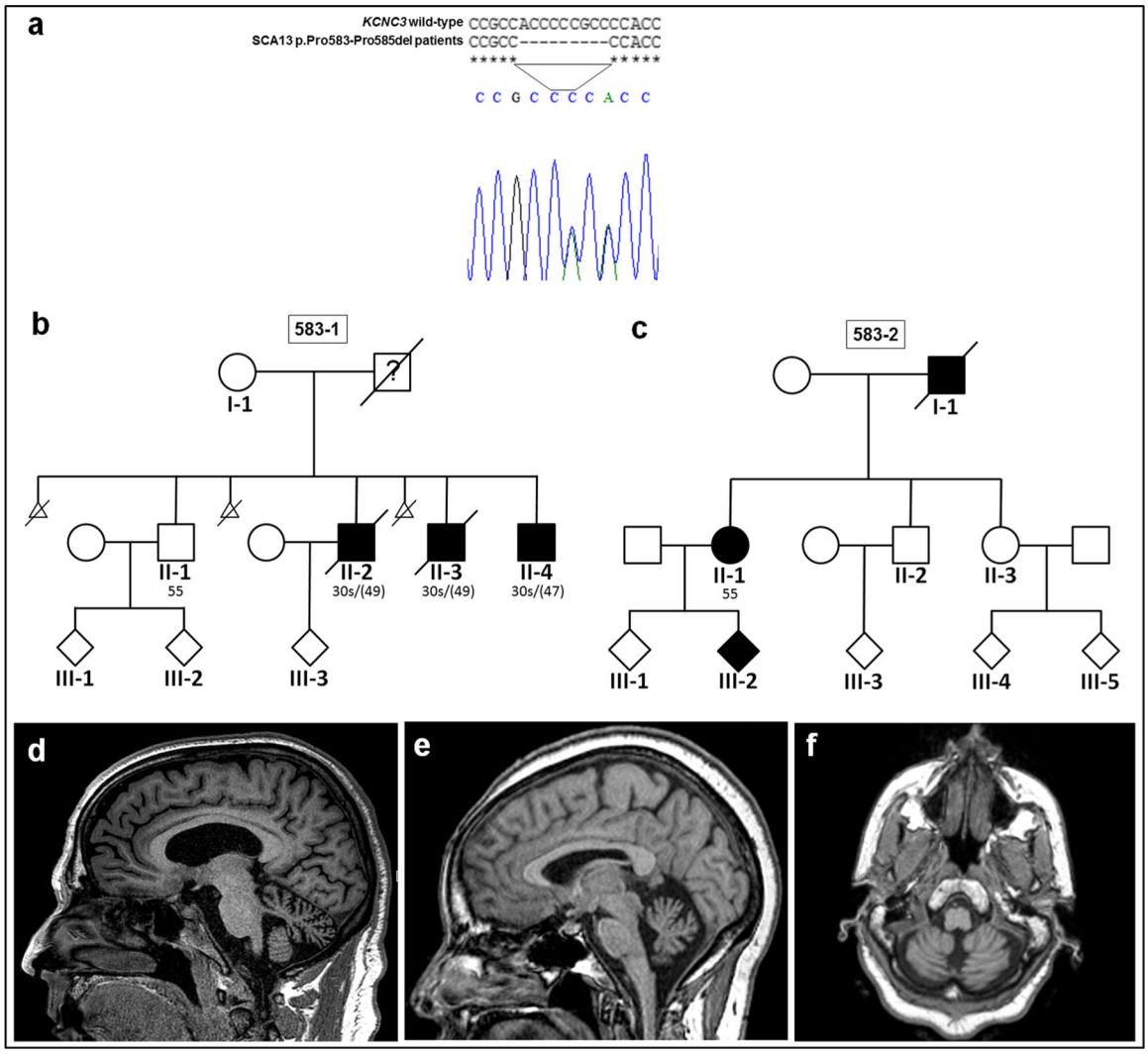

Fig. 1.

Pedigrees affected by the p.Pro583_Pro585del mutation, and MRIs of the brains of patients. (**a**) Chromatogram showing deleted nucleotides accounting for the loss of three proline residues in *KCNC3*. (**b**) Pedigree 583–1 of three brothers (II-2, II-3, and II-4) affected by the p.Pro583_Pro585del mutation. Age of clinical onset (years) indicated below symbols. Age of death (years) in parentheses. (**c**) Pedigree 583–2. Proband II-1 and her presymptomatic offspring were both positive for the p.Pro583_Pro585del mutation on genetic testing. (**d**) T1-weighted midsagittal brain MRI of proband 583–1, II-4, showing cerebellar atrophy. (**e**) T1-weighted midsagittal and (**f**) axial brain MRIs of proband 583–2, II-1, showing cerebellar atrophy

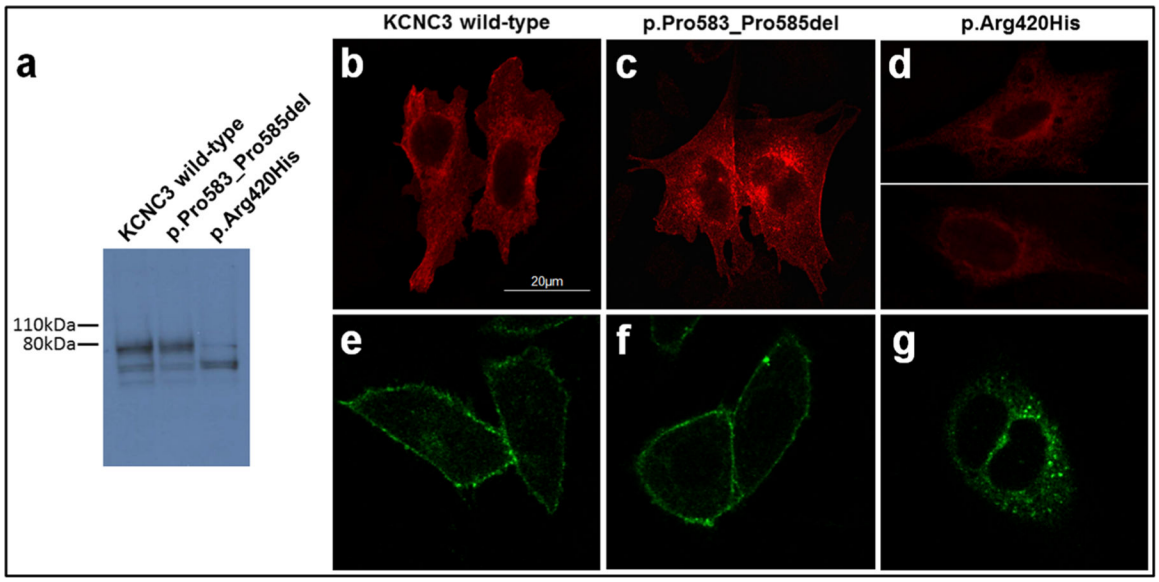

Fig. 2.

The p.Pro583_Pro585del mutant protein traffics normally, slows inactivation, and reduces sensitivity to actin depolymerization. (**a**) Immunoblot of protein extracted from CHO cells expressing KCNC3 or p.Pro583_Pro585del, showing normal glycosylation in contrast to abnormally glycosylated p.Arg420His. (**b–d**) Immunofluorescence of the three proteins showing normal trafficking of both KCNC3 and p.Pro583_Pro585del, as compared to intracellularly retained p.Arg420His. (**e–g**) Fluorescence imaging with Clover-tagged constructs confirming normal trafficking of KCNC3 and p.Pro583_Pro585del compared with intracellularly retained p.Arg420His

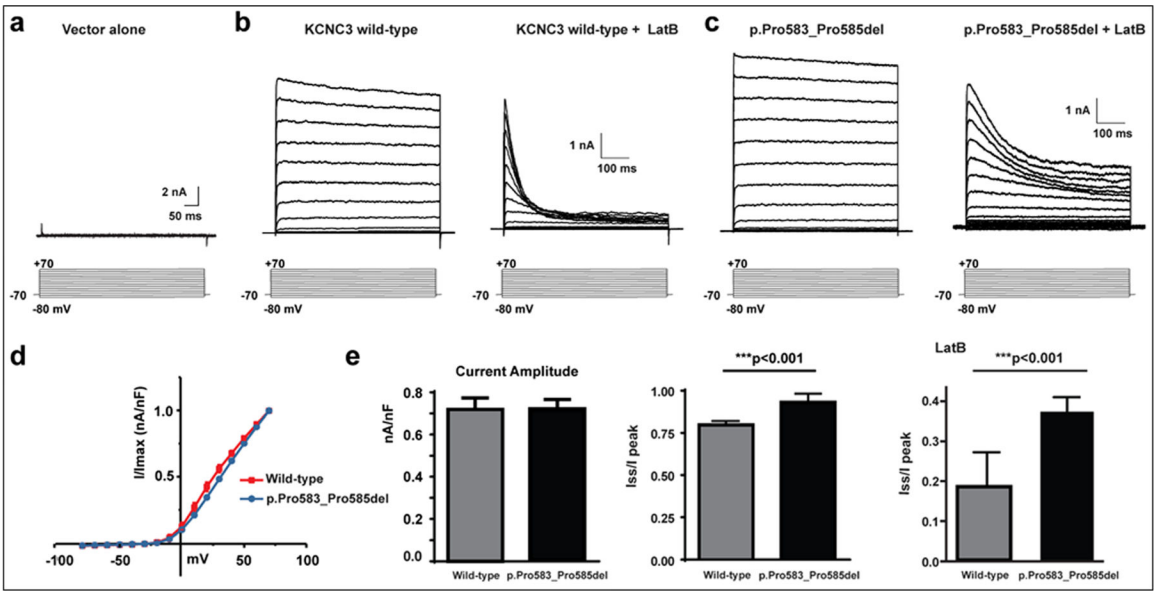

Fig. 3.

p.Pro583_Pro585del currents are resistant to latrunculin B. (**a**) Currents recorded from CHO cells expressing vector alone. Currents recorded from cells expressing (**b**) KCNC3 and (**c**) p.Pro583_Pro585del. Left traces are from untreated cells and red traces are from cells pretreated with 10 μM latrunculin B (LatB) for 1 h before recording. (**d**) Representative currents were evoked from a holding potential of − 70 mV to test potentials between − 80 to + 70 mV. (e) Bar graphs showing mean current densities and degrees of inactivation ± SEM at + 70 mV (steady state current/peak current, Iss/Ipeak) for wild-type Kv3.3 and for p.Pro583_Pro585del with or without LatB treatment. All bar graphs represent the means of n = 15–16 cells. Significance was determined using the two-tailed t test, with $p < 0.001$ represented as three asterisks